

Collective fluorescence and decoherence of a few nearly identical quantum dots

Anna Sitek and Paweł Machnikowski

Institute of Physics, Wrocław University of Technology, 50-370 Wrocław, Poland

We study the collective interaction of excitons in closely spaced artificial molecules and arrays of nearly identical quantum dots with the electromagnetic modes. We discuss how collective fluorescence builds up in the presence of a small mismatch of the transition energy. We show that a superradiant state of a single exciton in a molecule of two dots with realistic energy mismatch undergoes a two-rate decay. We analyze also the stability of subdecoherent states for non-identical systems.

I. INTRODUCTION

Confinement of carriers in semiconductor quantum dots (QDs) leads to spectrally isolated states which may be optically controlled at a high level of coherence^{1,2}. A single QD offers at most two degrees of freedom (a biexciton) which may be coherently manipulated by optical fields in various ways^{3,4}, allowing one to demonstrate the simplest non-trivial quantum logical operations. In order to overcome this two-qubit limitation one needs to develop manufacturing methods and control schemes for arrays of two and more QDs. Conditional control of such systems, indispensable in both classical and quantum computing schemes, requires interaction between the QDs in the array^{5,6}, which may be provided, e.g., by dipole interaction between confined excitons^{6,7}. Therefore, much experimental effort has been devoted to the investigation of the coupling between QDs and its signatures in the optical response and correlation statistics of quantum dot molecules (QDMs) built of two coupled QDs^{8,9,10,11,12}. It turns out that dephasing of excitons in QDMs differs considerably from that of individual QDs¹³.

Even without interaction, optical properties of QDMs and QD arrays may be strongly modified due to collective coupling of suitably closely spaced QDs to the electromagnetic (EM) field. These collective effects have been extensively studied for atomic systems^{14,15,16,17,18} where they manifest themselves by superradiant emission, i.e., an outburst of radiation from the excited sample, markedly different from any exponential decay¹⁹. On the other hand, the collective interaction leads to the appearance of subradiant states for which the probability amplitudes for photon emission interfere destructively, leading to decoupling from the EM reservoir and to infinite lifetime. It has been proposed to use these states for noiseless encoding of quantum information²⁰. For the analogous problem of coupling to phonon modes of a semiconductor, "subdecoherent states" of QD arrays have been suggested as a possible noiseless implementation²¹. Compared to atomic samples, QDs may be easier to arrange in a regular array but the perfectly identical transition energy characteristic of natural atoms is extremely hard to reach for these artificial systems.

The purpose of this paper is twofold. First, we deal with the general, theoretical problem of the stability

of collective interaction, including noiseless encoding, against variations of the transition energies. Second, we look for clear manifestations of interaction between the QDs in the experimentally observable optical properties of the QD arrays, depending on the difference (mismatch) of the transition energies of individual QDs.

Thus, we study the interaction between small, slightly inhomogeneous arrays of QDs and their EM environment. The system evolution is described within the Weisskopf-Wigner approach²². We show how the coherent interaction is destroyed by growing inhomogeneity of the transition energies in the regime where the latter is comparable to decay rate. As important examples, we discuss the buildup of superradiant emission from a few QDs and the decay of "subdecoherent" states built on non-identical QDs. We show that interaction between dots in a regular array may, to some extent, stabilize the coherence, in contrast to randomly distributed atomic systems, where it leads to dephasing¹⁵. We discuss also how the interplay of the transition energy mismatch and interaction strength determines the time evolution of the luminescence of a more realistic QDM. We show that the decay of luminescence varies from exponential with a single QD rate (for weakly interacting dots), through nonexponential (for interaction compared to energy difference), again to exponential with doubled rate (when interaction energy prevails).

The paper is organized as follows. In Section II we define the model used to describe the system. Section III describes the collective fluorescence and stability of quantum states in a molecule built of two dots. Next, in Section IV we extend the discussion to arrays of four dots. The final discussion and conclusions are contained in Section V.

II. THE SYSTEM

We consider an array of QDs located at points \mathbf{r}_i . We assume that each dot may either be empty or contain one ground state exciton of fixed polarization with an interband transition energy E_i , hence can be described as a two-level system. The dots interact with transverse EM modes with frequencies $\omega_k = ck$, where k is the wavenumber and c is the speed of light. We will describe the system in the interaction picture with respect to the

Hamiltonian $H_0 = \sum_j E_j \hat{n}_j + \sum_k \epsilon_k b_k^\dagger b_k$, ($\sim = 1$), where b_k ; b_k^\dagger are photon creation and annihilation operators (labels polarizations), E_j is the average of the energies E_j , and \hat{n}_j is the occupation operator for the j th dot, $\hat{n}_j = \sum_{\alpha} \hat{c}_{j\alpha}^\dagger \hat{c}_{j\alpha}$, where $\hat{c}_{j\alpha} = \sum_{\beta} i_{j\alpha\beta} \hat{\sigma}_{\beta}$ and $\hat{\sigma}_{\beta}$ are Pauli matrices acting on the j th two-level system. The Hamiltonian of the system is then $H = H_X + H_I$. The first component describes the excitons,

$$H_X = \sum_j E_j \hat{n}_j + \sum_{j \neq l} V_{lj} \hat{n}_j \hat{n}_l; \quad (1)$$

where $E_j = E_j - E$ are the energy deviations from the average and V_{lj} are Forster couplings between the QDs³⁴,

$$V_{lj} = \frac{1}{4 \epsilon_0 \epsilon_r r_{lj}^3} d^2 \frac{3 \hat{\mathbf{d}}_l \cdot \hat{\mathbf{d}}_j - 3 \hat{\mathbf{d}}_l \cdot \hat{\mathbf{r}}_{lj} \hat{\mathbf{r}}_{lj} \cdot \hat{\mathbf{d}}_j}{r_{lj}^5}; \quad r_{lj} = |\mathbf{r}_j - \mathbf{r}_l|;$$

where d is the interband dipole moment (for simplicity equal for all dots), ϵ_0 is the vacuum dielectric constant, and ϵ_r is the relative dielectric constant of the semiconductor. For self-assembled dots, typical values for this coupling range from eV for the distance r_{lj} of order of 100 nm to meV for closely stacked dots separated by 10 nm^{12,23,24}. Another contribution to the coupling may come from the polariton effect (coupling to transverse eld)²⁵.

The second term in the Hamiltonian accounts for the interaction with the EM modes in the dipole approximation and rotating wave approximation (RWA)

$$H_I = \sum_k \sum_j g_k e^{i(\mathbf{k} \cdot \mathbf{r}_j - E_j t)} b_k^\dagger + H.c.; \quad (2)$$

with $g_k = i d \cdot \hat{\mathbf{e}}(\mathbf{k}) \sqrt{\epsilon_0 \epsilon_r V}$, where $\hat{\mathbf{e}}(\mathbf{k})$ are unit polarization vectors and V is the normalization volume for EM modes³⁵. The QDs are placed at distances much smaller than the relevant photon wavelength so that the spatial dependence of the EM eld may be neglected (the Dicke limit). For wide-gap semiconductors with $E_g \gg 1$ eV, zero-temperature approximation may be used for any reasonable temperature.

In the present discussion, we disregard the coupling of the carriers with phonons. Let us note that the quantum confinement of excitons leads to a separation of at least a few meV between the ground exciton state involved in our analysis and the lowest excited state in a single dot. Therefore, no real-phonon-induced transitions may take place in a single dot as long as the temperature is low enough. It has been shown that the combination of dipole interaction and phonon coupling may lead to phonon-assisted Coulomb transfer between the dots²⁶, which might be responsible for the unidirectional transfer observed in the experiment¹². However, the estimated rate reaches its maximum of 2 ns for the energy separation of a few meV and decreases considerably away from this point²⁶. Therefore, we neglect this effect in the present considerations. For extremely closely spaced

dots, with strongly overlapping carrier wave functions, phonon-assisted tunneling²⁷ processes might also take place on time scales comparable to those characteristic of the radiative decay. Similar to the phonon-assisted Coulomb transfer, such processes would lead to thermalization of the state of a QDM or QD array which, in general, might suppress the dynamics described in the following sections.

Another phonon effect on the exciton state is pure dephasing^{28,29}. In QDMs, like in individual QDs, such processes affect only the first few picoseconds of the optical response of a QDM¹³, while our present discussion is focused on the radiative decay that develops at much longer times. Due to this separation of time scales, the evolution related to the radiative processes may be discussed separately from this pure dephasing effect. If the system state is prepared by an ultrafast pulse, the initial phonon dynamics may result in a certain reduction of the coherence of the initial state, as we qualitatively discuss in the following sections.

III. QUANTUM DOT MOLECULES (2 QDS)

We will start our discussion with quantum dot molecules composed of two QDs. In the present section, we will first discuss the decay of sub- and super-radiant single exciton states in terms of the formal quantum density with respect to the unperturbed state and in terms of the experimentally measurable exciton occupation. Then, we proceed to the decay of the biexciton state which will be studied again in terms of density and in terms of the measurable photon emission rate.

A. Single-exciton states

The RWA Hamiltonian conserves the number of excitations (excitons plus photons). Let us first consider the initial subradiant state $|j(0)\rangle = (|j1\rangle - |j0\rangle)/\sqrt{2}$, where the two-digit kets denote the occupations of the respective dots. Since there is only one excitation in this state it may, in general, evolve into

$$|j(t)\rangle = c_{01}(t)|j1\rangle + c_{10}(t)|j0\rangle + \sum_k c_{00k}(t)|j0;k\rangle;$$

where the last ket denotes the state with no excitons and with one photon in the mode $(\mathbf{k}; \lambda)$. The Schrodinger equation leads to the system of equations for the coefficients

$$i\dot{c}_{01} = c_{01} + V c_{10} + \sum_k g_k c_{00k} e^{i(E_j - \epsilon_k)t}; \quad (3a)$$

$$i\dot{c}_{10} = c_{10} + V c_{01} + \sum_k g_k c_{00k} e^{i(E_j - \epsilon_k)t}; \quad (3b)$$

$$i\dot{c}_{00k} = g_k (c_{01} + c_{10}) e^{i(E_j - \epsilon_k)t}; \quad (3c)$$

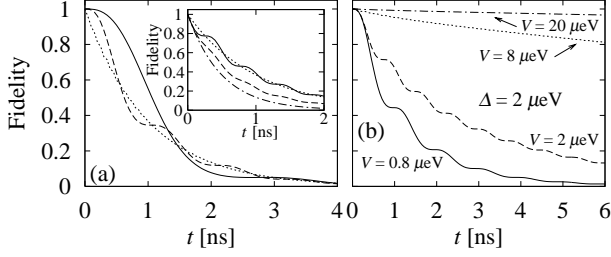


FIG. 1: (a) The fidelity for a subradiant state for $V = 0$ and $\Delta = 0.8$ eV (solid), 2 eV (dashed) and 20 eV (dotted). (b) The fidelity for $V \neq 0$, $\Delta = 2$ eV. Inset in (a) shows the fidelity of a superradiant state for different dots without interaction ($\Delta = 4$ eV, solid) and for interacting dots ($\Delta = 2.68$ eV, $V = 2.97$ eV, dashed), compared to an exponential decay with the rates Γ and 2Γ (dotted and dash-dotted, respectively).

where $V = V_{12}$ and $\Delta = E_2 - E_1$. Following the standard Weisskopf-Wigner procedure³⁰ we formally integrate Eq. (3c) and substitute to Eq. (3a,b), which yields

$$\dot{c}_{01;10} = -\frac{i}{Z} c_{01} - iV \bar{q}_0$$

$$+ \int_0^t ds R(s) (c_{01}(t-s) + \bar{q}_0(t-s));$$

where $R(s) = \sum_k \dot{\rho}_k \int d\mathbf{r} e^{i(E_1 - E_k)t}$ is the memory function of the photon reservoir. As the latter decays extremely quickly compared to the timescales of the evolution of $c_{01;10}$ one can perform the usual Markov approximation and neglect the s dependence under the integral. Using the fact that

$$\text{Re} \int_0^t ds R(s) = \frac{E^3 \dot{\rho}}{6 \pi_0 c^3} \frac{1}{2};$$

where $\dot{\rho}$ is the spontaneous decay rate (throughout the paper we set $\dot{\rho} = 1$ ns), neglecting the imaginary part (i.e., assuming that the Lamb shift and other radiative corrections are included in the energies), and denoting $c = (c_{10}; c_{01})^T$ one gets

$$\dot{c} = \hat{A}c; \quad \hat{A} = i \sigma_z - iV + \frac{\dot{\rho}}{2} \times \frac{1}{2} I; \quad (4)$$

where $\sigma_{x,z}$ are Pauli matrices and I is the unit matrix. The reduced density matrix for the charge subsystem may now be easily constructed as $\rho_{01;01} = \dot{\rho}_{01} \dot{\rho}_{10} = \dot{\rho}_{10} \dot{\rho}_{01}$, $\rho_{01;10} = \rho_{10;01} = c_{01} c_{10}$, $\rho_{00;00} = 1$, $\rho_{01;01} = \rho_{10;10}$, with all the other elements equal to 0.

In order to test the stability of the ideally subradiant state in the case of non-identical dots we denote by $j(t)$ the pure state evolving from $j(0) = |j\rangle$ in the absence of the EM reservoir ($\dot{\rho} = 0$) and denote the fidelity of the actual state by $F = \langle j(t) | j(t) \rangle$. In Fig. 1(a) we show the result for a few values of the energy difference in the limit of vanishing Forster coupling between the dots (i.e., for sufficiently distant dots). It is clear that

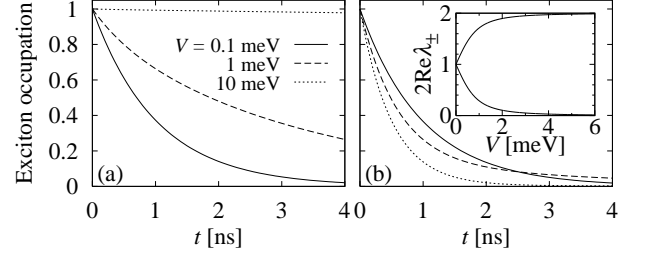


FIG. 2: The exciton occupation for sub- (a) and superradiant (b) states for $\Delta = 1$ meV. The inset in (b) shows the values of the occupation decay rates.

the state maintains its subradiant (stable) character until $t = (2\Gamma)^{-1}$ but then it enters a superradiant phase and the fidelity rapidly decays below the value corresponding to an exponential (uncorrelated) decay. Depending on the value of Δ , a certain number of oscillations around this uncorrelated decay rate may be observed. In the limit of large Δ these oscillations become very fast, their amplitude decreases, and the decay closely follows that of uncorrelated systems, as expected for systems with large energy difference and therefore interacting with disjoint frequency ranges of the photon reservoir. It is clear that observing collective effects for such non-interacting dots requires transition energies identical up to several eV.

If the QDs are close enough, the Forster interaction becomes effective. Since the sub- and superradiant states are eigenstates of the Forster Hamiltonian separated by an energy $2V$, the transition from the initially subradiant state to the superradiant state is suppressed if the magnitude of the Forster coupling exceeds the energy difference Δ . This is shown in Fig. 1(b). It is clear that the decay rate is reduced when $V \rightarrow \Delta$ and the subradiance is recovered for $V > \Delta$. Note that, apart from the trivial limiting cases, the decay is markedly non-exponential and its modulation yields information on the origin of the energy level splitting in the system. Indeed, the decay of the superradiant state $j(0) = (\dot{\rho}_{11} + \dot{\rho}_{10})/\sqrt{2}$ shown in the inset to Fig. 1(a) is clearly different for two systems with the same energy splitting, depending on whether the splitting originates from the difference between the dots or from the interaction.

The signatures of collective interaction with the electromagnetic field may also be found in the evolution of measurable quantities. As an example, let us consider the average number of excitons in the QDM. In the present state of the art of QD manufacturing, the differences between the transition energies of the two dots are rather in the meV than in the eV range discussed in the previous case. Therefore, let us consider the evolution of exciton occupations for the initial states $j(0) = (\dot{\rho}_{11} - \dot{\rho}_{10})/\sqrt{2}$ for a QDM with $\Delta = 1$ meV. The results are shown in Fig. 2. As can be seen, in this case the decay of the occupation shows no oscillations. For $V \rightarrow 0$, both states show simple exponential decay with the rate Γ . In the opposite limit, $V \rightarrow \Delta$, the subradiant state becomes

stable while the superradiant state decays exponentially with a twice larger rate. In the intermediate range of parameters, the decay is not exponential.

The superradiant state is particularly relevant for optical experiments since such a bright combination of single-exciton states is excited by ultrafast optical pulses from the ground state. Thus, the curves plotted in Fig. 2 directly correspond to the decay of population after an optical excitation.³⁶ Therefore, let us study this decay in more detail.

The system evolution is governed by the matrix \hat{A} [Eq. (4)] which, for $\gamma = 0$, is nearly purely anti-Hermitian. Therefore, its eigenvectors are nearly orthogonal to each other. Up to corrections of order of $\gamma = 1$, they can be written in the form

$$u_+ = \frac{\cos' \gamma}{\sin' \gamma}; \quad u_- = \frac{\sin' \gamma}{\cos' \gamma};$$

where

$$\sin' \gamma = \frac{1}{2} \sqrt{1 - \frac{1}{2 + \sqrt{2}}}; \quad \cos' \gamma = \frac{1}{2} \sqrt{1 + \frac{1}{2 + \sqrt{2}}}.$$

The corresponding eigenvalues are

$$\lambda_{\pm} = \frac{\gamma}{2} \sqrt{1 \pm \frac{1}{2 + \sqrt{2}}};$$

The solution of Eq. (4) for the superradiant initial condition is

$$c(t) = \sin'(\gamma + \lambda_+) u_+ e^{-\lambda_+ t} + \cos'(\gamma + \lambda_+) u_- e^{-\lambda_- t};$$

The number of excitons therefore evolves as

$$n(t) = |c(t)|^2 = \sin^2(\gamma + \lambda_+) e^{2\text{Re} \lambda_+ t} + \cos^2(\gamma + \lambda_+) e^{2\text{Re} \lambda_- t};$$

Due to the almost perfect orthogonality of the eigenvectors u_{\pm} the interference term vanishes and the occupation decay is a combination of two exponentials with different rates, as shown in Fig. 2(b). In the inset to this figure we show the values of the two decay constants as a function of V for $\gamma = 1$ meV.

If the initial sub- or superradiant state of a QDM is prepared by an ultrafast optical pulse it will partly lose its coherence within a few picoseconds of the system evolution due to phonon-induced pure dephasing. The detailed dynamics of this dephasing process differs from that of a single QD and depends on the system geometry³¹. Nonetheless, its essential effect is to perturb the superposition state towards a mixture of two states, each of which undergoes the usual exponential decay. Therefore, one may expect a decrease of the amplitude of the oscillations in Figs. 1 and 3 and a shift of the decay curves in Fig. 2 towards the monoexponential decay with the usual decay rate. For special values of the energy mismatch, the results may also be modified by the phonon-assisted Coulomb transfer²⁶.

B. Biexciton state

Next, let us consider the case of the same two QDs, but initially excited to the $|11\rangle$ state. This state can be experimentally prepared in various ways^{3,4}. The general form of the state is now

$$|j\rangle(t) = c_{11}(t) |11\rangle + \sum_k c_{01k}(t) |1k\rangle + \sum_k c_{10k}(t) |k0\rangle + \sum_{k,q} c_{00kq}(t) |0kq0\rangle;$$

and the amplitudes evolve according to the equations

$$i\dot{c}_{11} = \sum_k g_k (c_{01k} + c_{10k}) e^{i(E_k - E_{11})t}; \quad (5a)$$

$$i\dot{c}_{01k} = c_{01} + V c_{10} + g_k c_{11} e^{i(E_k - E_{11})t} + \sum_{q,q'} g_{q,q'} c_{00kq} e^{i(E_k - E_{q,q'})t}; \quad (5b)$$

$$i\dot{c}_{10k} = \sum_{q,q'} c_{10} + V c_{01} + g_k c_{11} e^{i(E_k - E_{11})t} + g_{q,q'} c_{00kq} e^{i(E_k - E_{q,q'})t}; \quad (5c)$$

$$i\dot{c}_{00kq} = g_{q,q'} (c_{01k} + c_{10k}) e^{i(E_k - E_{q,q'})t}; \quad (5d)$$

As previously, we formally integrate Eq. (5d), insert it into Eqs. (5b,5c), and use the short memory assumption. This yields the equation for $c_k = (c_{10k}; c_{01k})^T$,

$$\dot{c}_k = -i g \int_0^t ds \hat{A}(t-s) c_{11}(s) e^{i(E_k - E_{11})s} b; \quad (6)$$

where $b = (1; 1)^T$ and \hat{A} is defined in Eq. (4). Substituting this in turn into Eq. (5a) we find

$$\dot{c}_{11} = \int_0^t ds R(s) b^T e^{\hat{A}s} b c_{11}(t-s);$$

Since the elements of \hat{A} are of order of eV or meV, the matrix exponent is slowly varying on the timescales of reservoir memory, as is $c_{11}(t)$, and both may be taken at $s = 0$, which leads to the decay equation in the usual form $\dot{c}_{11} = -\gamma c_{11}$ or, for the corresponding element of the reduced density matrix, $\dot{\rho}_{11;11} = -2\gamma \rho_{11;11}$.

The evolution equations for the other elements of the density matrix may be found by writing, for instance, $\dot{\rho}_{01;01} = 2\text{Re} \sum_k (c_{10k} \dot{c}_{01k})$, substituting \dot{c}_{01k} from Eq. (6), and using once more the short memory approximation. Performing this procedure for all the elements of the single-exciton sector, one arrives at the equations

$$\begin{aligned} \dot{f}_{11} &= -2\gamma f_{11}; \\ \dot{f}_{10} &= (\text{Re} p + f_{10} - f_{11}) + 2V \text{Im} p; \\ \dot{f}_{01} &= (\text{Re} p + f_{01} - f_{11}) - 2V \text{Im} p; \\ \dot{p} &= 2i p - (p + \frac{f_{01} + f_{10}}{2} - f_{11}) \\ &\quad + iV (f_{01} - f_{10}); \end{aligned}$$

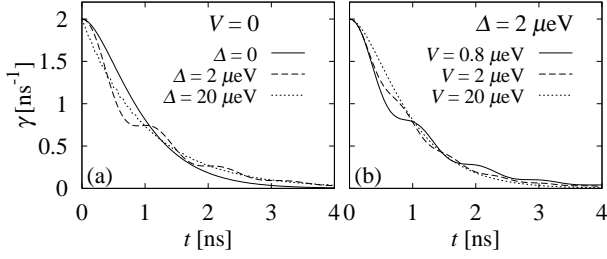


FIG. 3: Photon emission rate for a superradiant state for $V = 0$ (a) and for $V \neq 0$, $\Delta = 2$ eV (b).

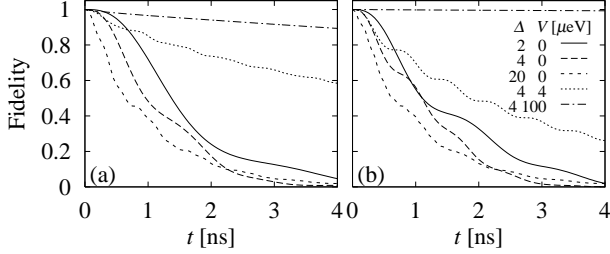


FIG. 4: The fidelity for two subradiant states j_{ai} (a) and j_{bi} (b) of 4 QDs for various combinations of parameters. The parameter values given in (b) are valid for both figures.

where we denoted $f_{lj} = \langle l_j | l_j \rangle$, $l, j = 0, 1$, and $p = \langle 01 | 10 \rangle$.

The photon emission rate $\gamma = (\mathcal{E}_{T1} + \mathcal{E}_{01} + \mathcal{E}_{T0})$ for the initial state j_{li} is plotted in Fig. 3. In the case of $V = 0$ [Fig. 3 (a)] we see that the photon emission loses its superradiant behavior for growing energy mismatch between the dots, tending to the usual exponential decay for large Δ . Like in the previous case, removing the degeneracy between the sub- and superradiant single-exciton states by including the Forster coupling stabilizes the collective fluorescence [the dotted line in Fig. 3 (b) coincides with the $\Delta = 0$ line in Fig. 3 (a)].

IV. QUANTUM DOT ARRAYS (4 QDS)

In this section, we study arrays of four QDs in a very special, regular arrangement. The resulting symmetry of the Forster term leads to symmetric eigenstates and, as we show below, to the stabilization of collective effects.

In general, the Weisskopf-Wigner equations lead to the Lindblad equation for the evolution of the reduced density matrix of the charge subsystem

$$\dot{\rho} = -i[H_X; \rho] + L[\rho]; \quad (7)$$

with

$$L[\rho] = \sum_j \left(\frac{1}{2} f_j + \dots \right); g_j;$$

where $f_j = \sum_i P_j^{(i)}$. We now use Eq. (7) to study the evolution of four QDs forming a square array in the xy

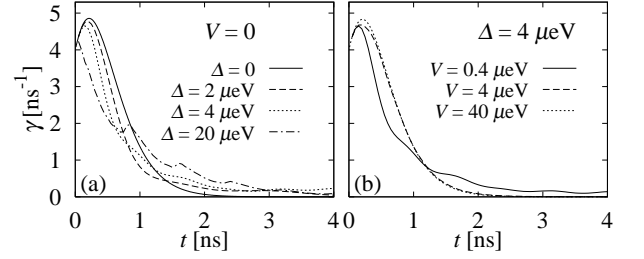


FIG. 5: Photon emission rate for a superradiant state of 4 QDs for $V = 0$ (a) and for $V \neq 0$ (b).

plane. The energy deviations of individual dots are now $\epsilon_i = \epsilon_i^0$, where $\epsilon_i^0 = 0$ and $\epsilon_i^2 = 1$, so that ϵ_i^2 is the mean square variation of the transition energies. The details of the system evolution depend on the particular choice of ϵ_i but the general behavior is only governed by the interplay of Δ and V (unless some particularly symmetric choice is made). We arbitrarily choose $\epsilon_1 = 0$, $\epsilon_2 = 0.8$, $\epsilon_3 = 0.27$, $\epsilon_4 = 0.54$ and use the mean square variation ϵ_i^2 as a parameter. The Forster interaction is parameterized by its magnitude V , with $V_{12} = V_{23} = V_{34} = V_{41} = V$ and $V_{13} = V_{24} = 2^{-3/2}V$ (the dots are numbered clockwise).

First, let us choose the subradiant initial states $j_a(0)i = (j_{1001i} - j_{101i} + j_{110i} - j_{1010i})/2$ and $j_b(0)i = (j_{1001i} - j_{1011i} + j_{110i} - j_{1100i})/2$, which span the subspace of logical qubit states that may be used for noiseless encoding of quantum information on four physical qubits²⁰. Obviously, for non-identical dots the phases in these superpositions will rotate and the state will be driven out of the initial noiseless subspace which leads to a decrease of fidelity, as shown in Fig. 4. Out of the two states, only $j_b(0)i$ is a non-degenerate eigenstate of the Frohlich interaction for the square array. As a result, as can be seen in Fig. 4, only this state is fully stabilized by the Forster interaction for V (the lines for $V = 100$ eV in Fig. 4 are very close to the asymptotic case of $V \rightarrow \infty$). Since the other state $j_a(0)i$ is never completely stable the entire "noiseless subspace" of logical states²¹ remains stable only for an extremely homogeneous array of QDs.

Finally, let us study the photon emission rate from a superradiant state of four excited QDs, $j(0)i = j_{1111i}$ (Fig. 5). Now, a clear superradiant peak of photon emission develops for identical dots but vanishes as the dots become different. Again, interaction between the dots in a regular array stabilizes the collective emission. It is interesting to note that the superradiant emission is close to ideal already for $V = 1$, while the subradiant states are stabilized only when the interaction exceeds the energy difference by an order of magnitude.

It should be stressed that the stabilization effect results from the special, highly symmetric arrangement of the QDs. It should be contrasted with the dephasing induced by analogous interactions in the randomly distributed atomic samples¹⁵. Likewise, in an irregular

ensemble of QDs obtained by spontaneous self-assembly no stabilization effect should be expected. However, recent progress in the pre-patterned and strain-engineered growth of QDs^{32,33} shows great promise for the manufacturing of QD arrays with a desired geometry.

V. CONCLUSIONS

We have shown that collective interaction of carriers in QDs with their EM environment is extremely sensitive to the homogeneity of the QD array. Already for the energy mismatch of order of μeV the sub- and superradiant behavior of physical quantities is replaced by their oscillation around the average exponential decay. Thus, observing collective fluorescence effects in an ensemble of non-interacting QDs seems highly unlikely. Likewise, implementing the noiseless encoding schemes requires the level of homogeneity much beyond the reach of the present

technology.

The destructive effect of inhomogeneity can be, to some extent, overcome by excitation-transfer coupling (Forster or tunneling) between the dots placed in a regular array. This can stabilize the subradiance of a state of 2 QDs and the superradiant emission from 4 QDs but (for a square alignment) still cannot assure stability of the entire noiseless subspace implemented on 4 QDs.

When the energy mismatch between the dots is of order of meV , like in the currently fabricated artificial molecules of two QDs, the oscillations disappear and one observes a decay of the excitation (exciton occupation number) composed of two exponentials. For such a realistic energy mismatch, the two decay rates for non-interacting dots are practically equal to the free decay rate. However, with growing interaction strength they approach 2 (superradiant component) and 0 (subradiant). Thus, their values carry information on the origin of the energy splitting (interaction vs. energy mismatch).

Electronic address: Pawel.Machnikowski@pwr.wroc.pl

- ¹ A. Zrenner, E. Beham, S. Stu er, F. F indeis, M. B ichler, and G. Abstreiter, *Nature* 418, 612 (2002).
- ² S. Stu er, P. Ester, A. Zrenner, and M. B ichler, *Phys. Rev. B* 72, 121301(R) (2005).
- ³ S. Stu er, P. Machnikowski, P. Ester, M. B ichler, V. M. Axt, T. Kuhn, and A. Zrenner, *Phys. Rev. B* 73, 125304 (2006).
- ⁴ X. Li, Y. Wu, D. Steel, D. Gammon, T. Stievater, D. Katzer, D. Park, C. Piermarocchi, and L. Sham, *Science* 301, 809 (2003).
- ⁵ E. Biolatti, R. C. Iotti, P. Zanardi, and F. Rossi, *Phys. Rev. Lett.* 85, 5647 (2000).
- ⁶ S. Sangu, K. Kobayashi, A. Shojiguchi, and M. Ohtsu, *Phys. Rev. B* 69, 115334 (2004).
- ⁷ L. Quiroga and N. F. Johnson, *Phys. Rev. Lett.* 83, 2270 (1999).
- ⁸ M. Bayer, P. Hawrylak, K. Hinzer, S. Fafard, M. Korkusinski, Z. R. Wasilewski, O. Stern, and A. Forchel, *Science* 291, 451 (2001).
- ⁹ T. U nold, K. M ueller, C. Lienau, T. Elsaesser, and A. D. Wieck, *Phys. Rev. Lett.* 94, 137404 (2005).
- ¹⁰ G. Ortner, M. Bayer, A. Larionov, V. B. Timofeev, A. Forchel, Y. B. Lyanda-Geller, T. L. Reinecke, P. Hawrylak, S. Fafard, and Z. Wasilewski, *Phys. Rev. Lett.* 90, 086404 (2003).
- ¹¹ H. J. Krenner, M. Sabathil, E. C. Clark, A. Kress, D. Schuh, M. B ichler, G. Abstreiter, and J. J. Finley, *Phys. Rev. Lett.* 94, 057402 (2005).
- ¹² B. D. Gerardot, S. Strauf, M. J. A. de Dood, A. M. Bychkov, A. Badolato, K. Hennessy, E. L. Hu, D. Bouwmester, and P. M. Petro, *Phys. Rev. Lett.* 95, 137403 (2005).
- ¹³ P. Borri, W. Langbein, U. Woggon, M. Schwab, M. Bayer, S. Fafard, Z. Wasilewski, and P. Hawrylak, *Phys. Rev. Lett.* 91, 267401 (2003).
- ¹⁴ H. M. Nussenzweig, *Introduction to Quantum Optics* (Gordon and Breach, New York, 1973).
- ¹⁵ M. Gross and S. Haroche, *Phys. Rep.* 93, 301 (1982).
- ¹⁶ R. H. Dicke, *Phys. Rev.* 93, 99 (1954).
- ¹⁷ R. H. Lehmberg, *Phys. Rev. A* 2, 883 (1970).
- ¹⁸ R. H. Lehmberg, *Phys. Rev. A* 2, 889 (1970).
- ¹⁹ N. Skribanowitz, I. P. Herman, J. C. MacGillivray, and M. S. Feld, *Phys. Rev. Lett.* 30, 309 (1973).
- ²⁰ P. Zanardi and M. Rasetti, *Phys. Rev. Lett.* 79, 3306 (1997).
- ²¹ P. Zanardi and F. Rossi, *Phys. Rev. Lett.* 81, 4752 (1998).
- ²² V. Weisskopf and E. Wigner, *Z. Phys.* 63, 54 (1930).
- ²³ B. W. Lovett, J. H. Reina, A. Nazir, and G. A. D. Briggs, *Phys. Rev. B* 68, 205319 (2003).
- ²⁴ K. J. Ahn, J. Forstner, and A. Knorr, *Phys. Rev. B* 71, 153309 (2005).
- ²⁵ G. Parascandolo and V. Savona, *Phys. Rev. B* 71, 045335 (2005).
- ²⁶ A. O. Govorov, *Phys. Rev. B* 71, 155323 (2005).
- ²⁷ V. Lopez-Richard, S. S. Oliveira, and G.-Q. Hai, *Phys. Rev. B* 71, 075329 (2005).
- ²⁸ B. Krummheuer, V. M. Axt, and T. Kuhn, *Phys. Rev. B* 65, 195313 (2002).
- ²⁹ A. Vagov, V. M. Axt, T. Kuhn, W. Langbein, P. Borri, and U. Woggon, *Phys. Rev. B* 70, 201305(R) (2004).
- ³⁰ M. O. Scully and M. S. Zubairy, *Quantum Optics* (Cambridge University Press, Cambridge, 1997).
- ³¹ A. Grodecka and P. Machnikowski, *Phys. Rev. B* 73, 125306 (2006).
- ³² H. Lee, J. A. Johnson, M. Y. He, J. S. Speck, and P. M. Petro, *Appl. Phys. Lett.* 78, 105 (2001).
- ³³ Y. Nakamura, N. Ikeda, Y. Sugimoto, H. Nakamura, S. Ohkouchi, and K. Asakawa, *Phys. Stat. Sol. (b)* 238, 237 (2003).
- ³⁴ For extremely closely spaced dots, the coupling will be dominated by tunnelling, which has the same structure as the Forster term.
- ³⁵ The full minimal-coupling Hamiltonian would yield a cutoff of g_k at $k_c = 1/l$, where l is the QD size. For our discussion it is only important that this frequency is extremely high, which justifies the Markov approximation. In this approximation, only the coupling at frequencies close to

is relevant for the radiative damping.

³⁶ Strictly speaking, the absence of the biexciton component requires either a large enough biexcitonic shift or an exci-

tation weak enough to neglect the higher-order biexcitonic occupation.